

Long Term Motion Prediction Using Keyposes

Sena Kiciroglu¹ Wei Wang^{1,2} Mathieu Salzmann^{1,3} Pascal Fua¹

¹ CVLab, EPFL, Switzerland

² University of Trento, Italy

³ ClearSpace, Switzerland

Abstract

Long term human motion prediction is an essential component in safety-critical applications, such as human-robot interaction and autonomous driving. We argue that, to achieve long term forecasting, predicting human pose at every time instant is unnecessary because human motion follows patterns that are well-represented by a few essential poses in the sequence. We call such poses “keyposes”, and approximate complex motions by linearly interpolating between subsequent keyposes. We show that learning the sequence of such keyposes allows us to predict very long term motion, up to 5 seconds in the future. In particular, our predictions are much more realistic and better preserve the motion dynamics than those obtained by the state-of-the-art methods. Furthermore, our approach models the future keyposes probabilistically, which, during inference, lets us generate diverse future motions via sampling.

1. Introduction

Human motion prediction is a key component of many vision-based applications, such as automated driving[12, 8], surveillance[21, 14], accident prevention[25], and human-robot interaction[11, 5]. It consists of forecasting the 3D articulated motion of a person in the future given the 3D poses corresponding to the previous few time instants. Much progress has recently been done in this field, thanks to the use of different deep learning strategies, such as recurrent neural networks [10, 18] and graph convolutional networks [28, 15, 27]. In essence, all of these methods treat motion prediction as the task of regressing a person’s pose in every future frame of a sequence. With 25fps videos, the number of frames grows quickly, and this approach has mostly been demonstrated for relatively short-term prediction, up to one second in the future. For safety-critical applications, however, such a short timespan might not suffice.

In this paper, we argue that predicting the pose in *every* future frame is unnecessary; given two poses separated by a short time interval, one can easily fill in the gap using simple linear interpolation between the two poses. We therefore

formulate motion prediction as the problem of generating a sequence of *keyposes*, which we define as the poses that are essential to reconstruct a complete motion by linear interpolation. Because keyposes are sparse in time, predicting them facilitates forecasting motion for longer timespans.

We then introduce an optimization-based strategy to extract such keyposes from the training data. While the training keyposes are typically unique, they still tend to be similar to each other because they represent motions depicting a relatively small set of activities. Instead of learning to regress to keyposes, we therefore cluster the training keyposes and turn motion prediction into a classification problem, where we predict to which cluster the future keyposes belong. In other words, we shift the focus on the transition from one keypose label to another. Moreover, by discretizing our predictions we also avoid accumulating errors, which prevents RNN-based methods from predicting longer timespans. Overall, this is quite reminiscent of what is being done in natural-language processing for machine translation, where tokens of words are generated from preceding tokens [29, 20].

To further encode the fact that the duration to transition between two keyposes may vary, we predict a value that encodes this duration. Given the predicted keypose labels and transition durations, we can recover the pose in each individual frame by linear interpolation.

In summary, our contributions are as follows.

- We introduce the concept of keyposes to represent human motion in a compact way.
- We propose a simple, yet effective strategy to extract meaningful keyposes from training data.
- We design a motion prediction framework that makes use of keyposes for long term prediction.
- We demonstrate that our approach can be used to predict diverse future motions given a single sequence of observation, an important property to account for uncertainty when forecasting at long-term horizons.

As will be shown by our experiments, our approach allows us to predict realistic motions for up to 5 seconds in the

future. In particular, compared to the state-of-the-art methods, which were designed for shorter timespans, the motions generated with our approach preserve the dynamic nature of the observations, whereas the SOTA ones tend to degenerate to static poses.

2. Related Work

The inherent complexity of human motion makes deep learning an ideal framework to tackle the motion prediction task. In this section, we first review the two main classes of deep models that have been used in the field and then discuss approaches that depart from these main trends.

2.1. Human motion prediction using RNNs

Recurrent neural networks (RNN) are widely used architectures for modeling time-series data, for instance for natural-language processing [29] and music generation [24, 23]. Since the work of Fragkiadaki *et al.* [9], these architectures have become highly popular for human motion forecasting. In this context, the S-RNN of Jain *et al.* [13] transforms spatio-temporal graphs to a feedforward mixture of RNNs; the Dropout Autoencoder LSTM (DAE-LSTM) of Ghosh *et al.* [10] synthesizes long-term realistic looking motion sequences; the recent Generative Adversarial Imitation Learning (GAIL) of Wang *et al.* [26] was employed to train an RNN-based policy generator and critic networks. HP-GAN [2] design an RNN-based GAN architecture to generate diverse future motions of 30 frames.

Despite their success, using RNNs for long-term motion prediction suffers from drawbacks. As pointed out by Martinez *et al.* [18] they tend to produce discontinuities at the transition between observed poses and predicted ones and often yield predictions that converge to the mean pose of the ground-truth data in the long term. In [18], this was circumvented by adding a residual connection so that the network only needs to predict the residual motion of the subject. Here, we also develop an RNN-based architecture. However, because we treat keypose prediction as a classification task, our approach will not suffer from the jitter that such models tend to generate when employed for regression.

2.2. Human motion prediction using GCNs

Mao *et al.* [28] proposed to overcome weaknesses of RNNs by encoding motion in DCT space, to model temporal dependencies, and learning the relationships between the different joints via a GCN. Lebailly *et al.* [15] build on top of this work by combining a GCN architecture with a temporal inception layer. The temporal inception layer serves to process the input at different subsequence lengths, so as to exploit both short-term and long-term information. Alternatively, “History Repeats Itself” [27] combines the GCN architecture with an attention module aiming to learn the

repetitive motion patterns. These methods constitute the state of the art for long-term prediction. Nevertheless, they were only showcased for forecasting up to 1 second in the future. As will be shown by our experiments, for longer timespans, they tend to degenerate to static predictions.

2.3. Other approaches to human motion prediction

Several other architectures have been proposed for human motion prediction. For example, Bütetage *et al.* [4] employ several fully-connected encoder-decoder models to encode different properties of the data. One of the models is a time-scale convolutional encoder, with different filter sizes. In [5], a conditional variational autoencoder (CVAE) is used to probabilistically model, predict and generate future motions. This probabilistic approach is extended in [6] to incorporate hierarchical action labels. Aliakbarian *et al.* [1] also perform motion generation and prediction by encoding their inputs using a CVAE. They are able to generate diverse motions by randomly sampling and perturbing the conditioning variables. Li *et al.* [16] use a convolutional neural network for motion prediction, producing separate short-term and long-term embeddings. In [7], interactions between humans and objects in the scene are learned for context-aware motion prediction, which enables predictions of up to 2 seconds. In any event, all the above-mentioned methods aim to predict the future poses at every time instant. Here, we will show that this is unnecessary, and that truly long-term prediction can be achieved more accurately by focusing the prediction on the essential poses, or keyposes, in a sequence.

3. Methodology

Classically, the task of motion prediction is defined as producing the sequence of 3D poses from $t = 1$ to $t = N$, denoted as $\mathbf{P}_{1:N}$, given the sequence of poses from $t = -M$ to $t = 0$, denoted as $\mathbf{P}_{-M:0}$. Each pose value \mathbf{P}_t is of dimension $3 \times J$, where J is the total number of joints. Therefore, pose-to-pose prediction can be written as

$$\mathbf{P}_{1:N} = F(\mathbf{P}_{-M:0}),$$

where F is the prediction function.

Our approach departs from this classical formalism by predicting keyposes from keyposes. A keypose \mathbf{K}_i is defined as a triplet containing a keypose value, label and duration, denoted as (\mathbf{V}_i, l_i, d_i) , where $i \in [1, I]$, where I is the total number of keyposes in a sequence. Each keypose value \mathbf{V}_i is of dimension $3 \times J$. Let us assume for now that we have extracted keypose values for the training data, and that we have clustered these keypose values into C clusters. We will discuss in Section 3.1 our approach to doing so. Then, the keypose label $l_i \in [1, C]$ indicates which cluster

the keypose falls into. Finally, the duration d_i is the number of transition frames from \mathbf{K}_i to \mathbf{K}_{i+1} .

Therefore, our keypose-to-keypose framework takes as input a motion $\mathbf{P}_{-M:0}$ defined by its keyposes $\mathbf{K}_{-I_1:0}$, where I_1 is the number of keyposes in the past sequence. We then aim to predict $\mathbf{K}_{1:I_2}$, where I_2 is the number of keyposes in the future sequence. We write this as

$$\mathbf{K}_{1:I_2} = G(\mathbf{K}_{-I_1:0}),$$

where G is the keypose-to-keypose prediction function.

In practice, we do not predict the keypose values $\mathbf{V}_{1:T_2}$, but only the labels $l_{1:T_2}$. To then obtain the d_i poses between keyposes \mathbf{K}_i and \mathbf{K}_{i+1} , we perform linear interpolation between the keypose cluster centers \mathbf{C}_{l_i} and $\mathbf{C}_{l_{i+1}}$. This yields

$$\mathbf{P}_{\Delta t+t} = \mathbf{C}_{l_i} + \Delta t \frac{\mathbf{C}_{l_{i+1}} - \mathbf{C}_{l_i}}{d_i}$$

where t is the time index of keypose \mathbf{K}_i in the sequence.

Note that we use a 3D-joint position representation of human motion. This representation has been gaining popularity over Euler angles, due to the latter suffering from ambiguities. Specifically, two different sets of angles can represent the same pose. Consequently, the interpolation between poses represented by angles becomes ambiguous as well.

Recent approaches have tried to solve this by changing the encoding to quaternions [22], but many works nonetheless report results using the 3D-joint position representation [28, 15, 27].

3.1. Keyposes

Given a sequence of poses \mathbf{P}_t , $t \in [1, T]$ where T is the length of the sequence, we seek to retrieve the keyposes \mathbf{K}_i , $i \in [1, I]$. We employ an optimization based strategy to determine the poses which minimizes the L2 error between the original sequence \mathbf{P} and the sequence reconstructed by linear interpolation.

Our method is as follows:

- We set \mathbf{P}_1 and \mathbf{P}_T to be the keyposes.
- We recursively subdivide the time window spanned by \mathbf{P} , where each split selects a pose \mathbf{P}_t at position t which has the highest L2 error to the pose reconstructed by linear interpolation at the same time index. The recursion ends once the error is below a threshold and we have an initial set of keyposes.
- The set of keyposes is further refined by optimizing for the time indices of the keyposes and the keypose values themselves. The optimization aims to minimize the L2

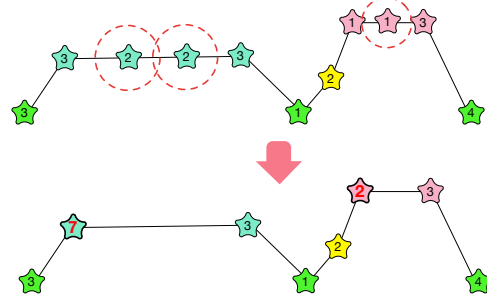


Figure 1. **Illustration of keypose pruning.** The top figure depicts the sequence before pruning. The keyposes are shown as stars, with their color indicating their label and the number inside indicating their duration. The keyposes to be pruned are circled. The bottom figure shows the sequence after pruning. The keyposes preceding the pruned ones have increased duration. Note that the same sequence can be reconstructed from both the pruned and unpruned keyposes, as there is no loss of information.

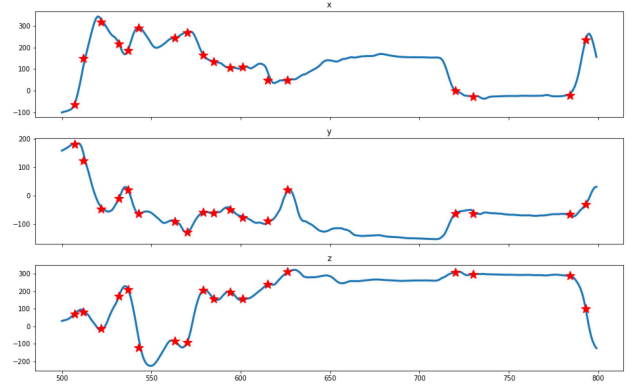


Figure 2. **Distribution of keyposes** in a short sequence. The plots depict the x, y, and z coordinates of the right wrist of subject 1 during the smoking action. We depict the locations of the keyposes as red stars. The keyposes are distributed more where the motion is the most varied and these keyposes have quite short duration.

error between the original sequence and the sequence reconstructed by interpolating the keyposes.

The keyposes are extracted for every training motion individually and collected in one set which is then clustered into 150 clusters via k-means. Each keypose is given a label determined by the cluster they are assigned to. Finally, we prune the keyposes by removing the unnecessary intermediate keyposes that have the same label as their preceding and succeeding keypose. Pruning is illustrated in Figure 1.

An example distribution of keyposes in a sequence can be seen in Figure 2.

3.2. Motion Prediction Framework

We have designed an RNN based neural network as our keypose-to-keypose prediction framework, as shown in Fig-

ure 3. The input to the network for step i are the pairs of tokenized keypose labels L_i and the keypose duration distribution D_i . We tokenize the labels via the following steps:

1. If we know the keypose value: We compute the negative distances of the keypose value V_i , $i \in [1, T]$, to all cluster centers C_j , $j \in [1, C]$.
2. If we do not know the keypose value (during inference): We compute the negative distances of the keypose cluster center of label i , C_{l_i} , $i \in [1, T]$, to all cluster centers C_j , $j \in [1, C]$.
3. We pass the resulting negative distances through a softmax operation with a temperature of 0.03.

Note that tokens sum up to 1 and can be thought of as a probability distribution over labels.

The durations are categorized as well into very short (less than 4 frames), short (between 5 and 8 frames), medium (between 9 and 12 frames), long (between 12 and 16 frames), and very long (more than 20 frames).

The network predicts a pair of distributions: over the labels and over the categories of durations. We train the network using three different losses:

- E_{KL} : the KL-divergence between the ground truth tokenized label and the predicted distribution over the labels,
- E_{ce} : the cross-entropy loss between the ground truth label and the predicted label distribution
- $E_{duration}$: the cross-entropy loss between the predicted duration category and the ground truth duration category.

The overall loss is

$$E = w_{KL}E_{KL} + w_{ce}E_{ce} + w_{dur}E_{duration} \quad (1)$$

where w_{KL} , w_{ce} , w_{dur} are the weights corresponding to the different loss terms. Both KL divergence and cross-entropy loss are used for classification, since the cross-entropy serves more as a hard loss on the predicted labels and the KL divergence serves more as a soft loss.

The loss is not only enforced on future predictions, it is also enforced on the outputs of the network as it processes the conditioning ground truth. For these past timesteps, the loss is multiplied by a factor of i/I_1 , where i is the prediction step and I_1 is the amount of past keyposes in the sequence. This factor is small in the beginning of the sequence, where we do not have enough past frames to base the future prediction on. As the amount of past frames increase, the loss factor gets larger, until it reaches 1.

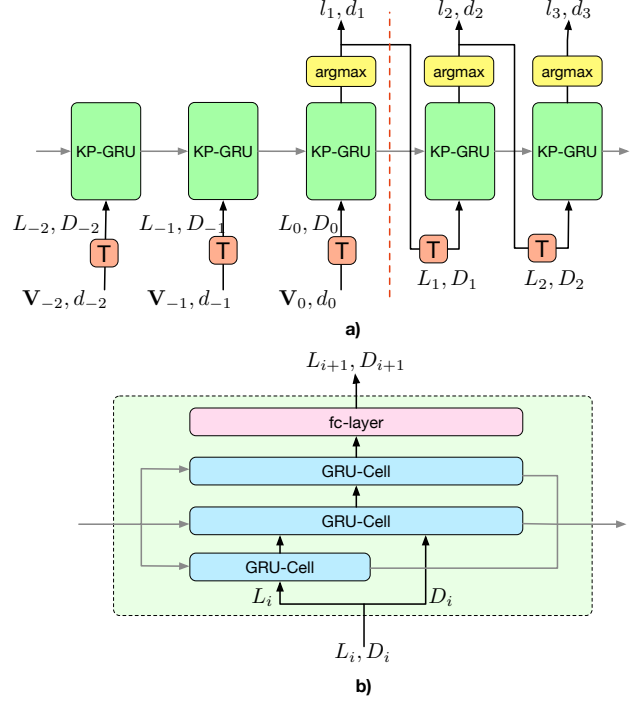


Figure 3. **Keypose-to-keypose network structure.** Figure a) depicts our overall architecture. At step i , pairs of tokenized keypose labels and durations, L_i, D_i are fed to the keypose GRU (KP-GRU) unit and the labels and durations of step $i + 1$ are predicted. The present is depicted at $i = 0$. Before this time-step, the network is given ground truth keyposes as conditioning. The tokenized label L_i is found using the keypose value V_i . After time-step $i = 0$, the network is given its own predictions as input rather than the ground truth. The tokenized label L_i is found using the predicted label l_i . The orange T blocks represent the tokenization operation. Figure b) depicts the inner structure of the KP-GRU unit, which consists of a three layer GRU network followed by a fully connected layer.

The label of the next keypose l_{i+1} is determined as the one with highest predicted probability. This label is tokenized before being fed back to the network. This procedure prevents error accumulating as the prediction progresses and guarantees that the network will never see anything very different from what it was trained on. The duration of the next keypose d_{i+1} is determined similarly: according to the category with the highest probability the following value is assigned: 3 for very-short, 6 for short, 10 for medium, 16 for long, and 25 for very long.

3.3. Diverse Motion Prediction

Our framework is designed to predict the tokens of the keypose labels, which can be likened to probability distributions. Therefore, during inference time, instead of choosing the label with the largest probability, we can sample the next label from the predicted distribution. Before sampling, the predicted distribution is smoothed via softmax with a

temperature of 0.1.

3.4. Implementation and Training Details

We use a 3 layer GRU, depicted in Figure 3. The GRU cells all have hidden states of size 1000. A Gaussian noise of magnitude 0.05 is added after the tokenization operation during training, to increase robustness and prevent overfitting. Also, in order to gradually teach the network to process its own samples, we use scheduled sampling for teacher forcing, as proposed in [3]. We train using 150 clusters, observing 8 keyposes in the past and predicting 12 keyposes in the future. During test time, we predict until we reach 5 seconds. The weights of the loss terms are set to $w_{KL} = 1.0$, $w_{ce} = 0.1$, $w_{dur} = 0.1$. Our network is trained for 800 epochs using a batch size of 64. We report the results of the model with the lowest validation loss. We use an Adam optimizer with learning rate 0.001 and 0.01 weight decay. The learning rate is decreased by a factor of 0.5 when the validation loss plateaus.

4. Experimental results

4.1. Datasets

Human3.6M is a standard 3D human pose dataset and has been widely used in the motion prediction literature [19, 13, 28]. It contains 15 actions performed by 7 subjects. The actions are *walking, eating, smoking, discussion, directions, greeting, phoning, posing, purchases, sitting, sitting down, taking photo, waiting, walking dog and walking together*. Human pose is represented using the 3D coordinates of 32 joints. As previous work [28, 15, 27], we load the exponential map representation of the dataset, remove global rotation and translation, and generate the Cartesian 3D coordinates of each joint mapped onto a uniform skeleton. Subject 5 is reserved for testing, subject 11 for validation and the remaining subjects are used for training. We test each method on the same 256 sequences formed using Subject 5’s randomly selected keypose indices.

4.2. Baselines

We select the following baselines for comparison: Mao *et al.* (HisRep) [27] and Lebailly *et al.* (TIM-GCN) [15], as they constitute the SOTA works designed for long-term prediction. For HisRep, we evaluate two versions. The first one, HisRep10, was presented as the best model. This model is trained to output 10 frames and iteratively use the predicted frames as input for the longer term future. We also evaluate HisRep125, which directly predicts 125 frames by taking 150 past frames as input. For TIM-GCN, we evaluate two versions as well. The first one is TIM-5-10-15, which observes subsequences of lengths 5, 10 and 15 and was reported to give the best performance for long-term predictions. We have also designed TIM-10-25-50, which ob-

serves subsequences of lengths 10, 25 and 50, making the architecture tailored for longer-term predictions of 5 seconds. Both versions of TIM-GCN were trained to predict 125 frames.

4.3. Metrics

Very long term prediction, as we tackle, is difficult to evaluate, as one may predict a plausible long-term future that nonetheless diverges from the real one. Therefore, direct comparison to the ground truth is ill-suited. Instead, we propose to evaluate the realism of the generated motion by passing it through an action classifier, as previously done in [10]. The classifier predicting the correct action class is a good indicator of the quality of the generated motion. We utilize two types of action classifiers: the ”motion-only” action classifier (MOAC) and the ”full” action classifier (FAC).

For FAC, we use the architecture of Li *et al.* [17], a state-of-the-art action classifier based on 3D pose sequences. This architecture takes as input the sequence of poses and the sequence of ”motions” which are the differences between consecutive poses. For MOAC, we use the same architecture with only the motion stream. A figure depicting the two architectures can be found in the supplementary material.

The purpose of using MOAC is to specifically evaluate the quality of the *motions*, which are the differences between consecutive poses. Our reasoning is to have a separate classifier that is not influenced by cues from a few well-predicted frames as our goal is for the entire predicted motion to be plausible.

4.4. Results

We present the results of the MOAC classifier in Table 1. Indeed, the results indicate that our method is better at predicting realistic motions. We believe the reason HisRep and TIM-GCN give worse results is that, especially for acyclic motions, they tend to produce very static results.

We provide qualitative results in Figure 4 for the smoking, sitting, discussion and walking actions. Our method tends to outperform the SOTA works for acyclic motions. For smoking and discussion, for example, our method generates much wider hand gestures than the SOTA works, which produce mostly static hands. For cyclic motions, such as walking, all methods are able to produce dynamic motions.

The results of the FAC classifier are provided in Table 2. We achieve comparable results to the SOTA, especially for top-2, top-3 and top-5 accuracies. However, we find this metric to be easily fooled by accurately predicted static poses. Indeed, the static predictor, which predicts a static pose chosen from the ground truth future poses for 5 seconds is also able to achieve quite high FAC accuracies,

| | top-1 | top-2 | top-3 | top-5 |
|--------------|-------------|-------------|-------------|-------------|
| oracle | 0.52 | 0.70 | 0.80 | 0.89 |
| TIM-5-10-15 | 0.13 | 0.20 | 0.31 | 0.49 |
| TIM-10-25-50 | 0.14 | 0.23 | 0.33 | 0.50 |
| HisRep10 | 0.19 | 0.30 | 0.39 | 0.54 |
| HisRep125 | 0.15 | 0.25 | 0.36 | 0.52 |
| Ours | 0.26 | 0.40 | 0.51 | 0.65 |

Table 1. **Results of the motion-only action classifier (MOAC).** We compare the classification accuracies of the motion predicted via our work (KP-network) compared to various versions of HisRep[27] and TIM-GCN[15]. We also report the accuracies of the oracle, which evaluates ground truth future motions, as an upper bound. We report the top-1, top-2, top-3 and top-5 accuracies. The results indicate that the motion predicted by our keypose network is more realistic than the motion predicted by the competing methods.

despite being severely handicapped. However, since it has no motion, its MOAC accuracies are on par with random selection. This check allows us to see that even with one accurately predicted pose, one is able to achieve high FAC accuracies.

| | top-1 | top-2 | top-3 | top-5 |
|--------------|-------------|-------------|-------------|-------------|
| oracle | 0.57 | 0.74 | 0.84 | 0.92 |
| static | 0.24 | 0.37 | 0.48 | 0.63 |
| TIM-5-10-15 | 0.35 | 0.48 | 0.57 | 0.72 |
| TIM-10-25-50 | 0.36 | 0.51 | 0.60 | 0.73 |
| HisRep10 | 0.35 | 0.49 | 0.59 | 0.74 |
| HisRep125 | 0.37 | 0.51 | 0.61 | 0.73 |
| Ours | 0.32 | 0.49 | 0.60 | 0.73 |

Table 2. **Results of the full action classifier (FAC).** We compare the classification accuracies of the motion predicted via our work compared to SOTA methods. The oracle evaluates ground truth future motions. Static evaluates a sequence consisting of a static pose from the future ground truth. Its relatively high performance despite being severely handicapped indicates that this is not a very reliable metric. HisRep125 achieves the best performance on FAC.

Additional qualitative results can be found in the supplementary material.

4.4.1 Diverse Motion Generation

We present the results of our diverse motion generation in Figure 5. We have observed that our method is capable of generating diverse, yet still meaningful motions. The average MOAC accuracies of the diverse motions are on par with the accuracies without sampling.

4.4.2 Analysis of Keypose Retrieval Methods

We evaluate the effect of using keyposes obtained via different strategies: sampling, clustering and ours. The naive-sampling method evenly samples the motion at a rate of

12 frames, which is the average keypose duration from our method. The keyposes are then clustered. There is no keypose pruning. This method also doesn’t require predicting durations, as the duration will always be 12. The clustering method performs clustering on *every* pose in the sequence, rather than only the poses indicated by the optimization results. Afterwards, the keyposes are pruned in the same manner as our method.

As can be seen in Table 3, our keypose method achieves the highest MOAC accuracies. The comparison with the naive-sampling method emphasizes the importance of having varying duration keyposes, as opposed to evenly sampling the motion. The comparison with the clustering method emphasizes the importance of optimizing for the keyposes.

| | top-1 | top-2 | top-3 | top-5 |
|----------------|-------------|-------------|-------------|-------------|
| Naive-sampling | 0.09 | 0.19 | 0.28 | 0.44 |
| Clustering | 0.12 | 0.21 | 0.31 | 0.46 |
| Ours | 0.26 | 0.40 | 0.51 | 0.65 |

Table 3. **Analysis on the method of obtaining keyposes.** We compare the MOAC accuracies of different keypose methods: naive-sampling, clustering and ours. The method we currently use achieves significantly higher classification accuracies than the other two methods, indicating that the quality of the keyposes affects the performance.

4.4.3 Ablation Study On Losses

We train our model either without the KL divergence loss or without the cross entropy loss and present the resulting performances in Table 4. We find that all the loss terms are useful for achieving higher MOAC accuracies.

| | top-1 | top-2 | top-3 | top-5 |
|-------------|-------------|-------------|-------------|-------------|
| w/o KL-loss | 0.11 | 0.23 | 0.31 | 0.47 |
| w/o ce-loss | 0.23 | 0.38 | 0.52 | 0.67 |
| Ours | 0.26 | 0.40 | 0.51 | 0.65 |

Table 4. **Ablation study on the different loss functions.** We present the results of MOAC without using the KL-divergence loss, without using the cross-entropy loss and using both losses. The performance degrades dramatically when we remove the KL-divergence loss. Cross-entropy loss seems less crucial, but gives us a boost in top-1 and top-2 classification accuracies.

5. Discussion & Conclusion

To the best of our knowledge, our work constitutes the first attempt to predict diverse futures for long-term durations of 5 seconds. Our method is built on predicting pairs of keypose labels and durations. Using these, we reconstruct the motion via linear interpolation. To evaluate our results, we have introduced a new action classifier, MOAC,

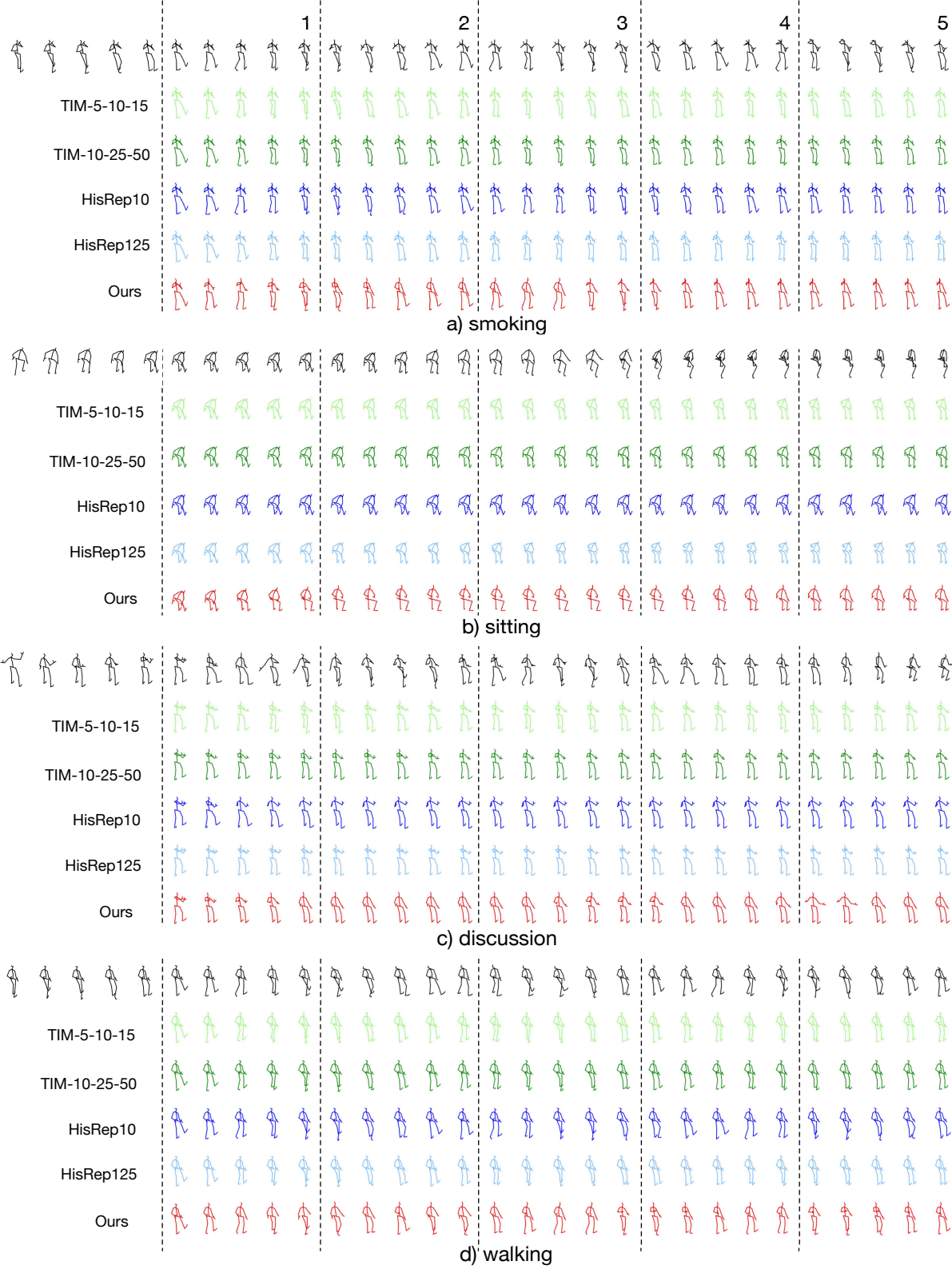


Figure 4. **Qualitative evaluation of our results** compared to the SOTA works, light green: TIM-5-10-15, dark green: TIM-10-25-50, dark blue: HisRep10, light blue: HisRep125, red: Ours. The top black row depicts the ground truth, and the first 5 poses are the conditioning ground truth. The numbers at the top indicate the future timestamp in seconds. We observe that we produce more dynamic poses. It is especially evident for smoking and discussion, as we can see that the hands are making wide gestures in our predictions, whereas for the SOTA works they are more static. For cyclic motions such as walking, the SOTA works also produce dynamic motions.

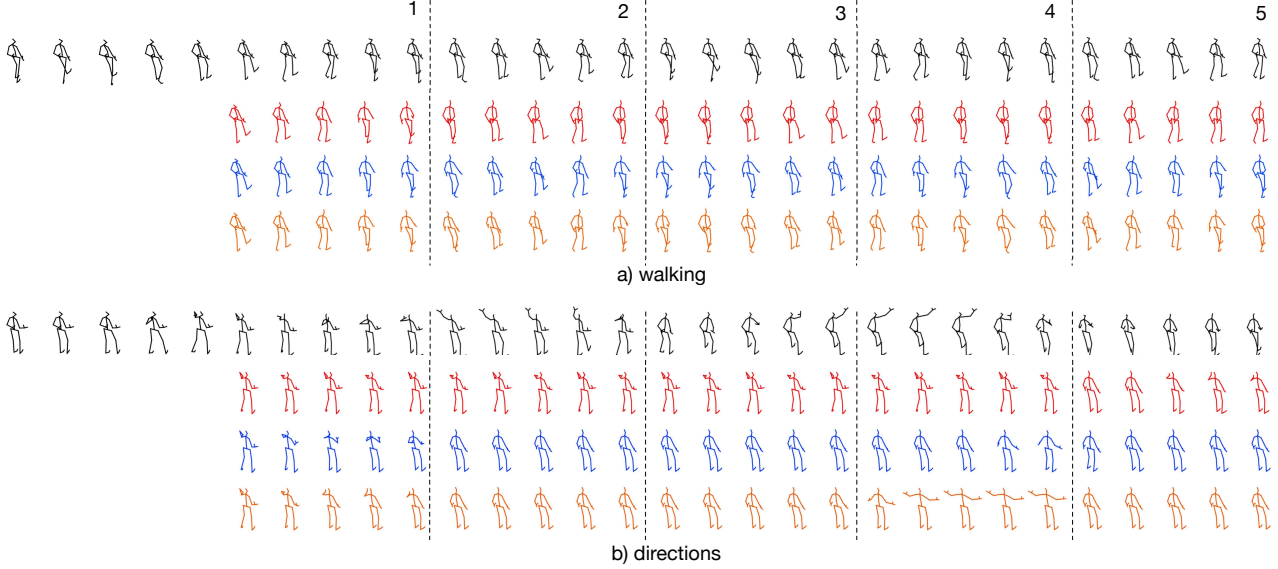


Figure 5. **Qualitative results of our diverse motion prediction** obtained through sampling the predicted label distribution. The numbers at the top indicate the timestamp in seconds. The top row in black depicts the ground truth, and the remaining rows in color are our generated motions. The sampled motions are quite diverse, yet can still be classified as “walking” and “directions”.

that specifically focuses on the transitions between poses, thus placing an emphasis on the correctness of the *motion*, rather than the *poses*. We have observed that compared to recent SOTA works tailored for learning patterns for long term predictions, we achieve more dynamic and realistic poses. We also demonstrate that we can easily sample diverse future motions using our method.

We have noticed that the biggest handicap of our approach comes from its biggest strength: our use of cluster centers for motion prediction. While quite powerful, these cluster centers cannot perfectly model all the poses. Different methods of clustering can be tried for improved performance. We also present failure cases in Figure 6, due to incorrect label prediction. As future work, we plan to focus on resolving these issues by expanding to architectures better-tailored for processing long sequences, such as transformer networks.

References

- [1] Sadegh Aliakbarian, Fatemeh Sadat Saleh, Mathieu Salzmann, Lars Petersson, and Stephen Gould. A stochastic conditioning scheme for diverse human motion prediction. In *Conference on Computer Vision and Pattern Recognition*, 2020. 2
- [2] Emad Barsoum, John Kender, and Zicheng Liu. HP-GAN: probabilistic 3d human motion prediction via GAN. *Conference on Computer Vision and Pattern Recognition Workshops*, 2017. 2
- [3] S. Bengio, O. Vinyals, N. Jaitly, and N. Shazeer. Scheduled Sampling for Sequence Prediction with Recurrent Neural Networks. In *Advances in Neural Information Processing Systems*, 2015. 5
- [4] J. Butepage, M.J. Black, D. Kragic, and H. Kjellstrom. Deep Representation Learning for Human Motion Prediction and Classification. In *Conference on Computer Vision and Pattern Recognition*, 2017. 2
- [5] Judith Bütage, Hedvig Kjellström, and Danica Kragic. Anticipating many futures: Online human motion prediction and generation for human-robot interaction. In *ICRA*, 2018. 1, 2
- [6] J. Bütage, H. Kjellström, and D. Kragic. Predicting the

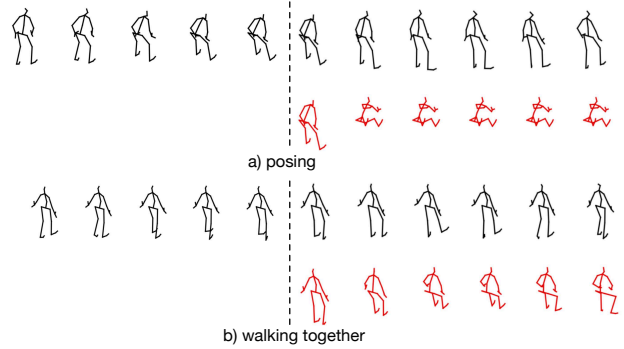


Figure 6. **Examples of failure** to predict the correct keypose labels. The top example is from the category “posing”, however once our model detects that the person is leaning down, it switches to dog-petting motion resembling the poses from the “walking dog” category. The bottom example depicts our network predicting labels belonging to the “sitting” category, even though the past poses are from the category “walking together”.

- what and how - a probabilistic semi-supervised approach to multi-task human activity modeling. In *2019 IEEE/CVF Conference on Computer Vision and Pattern Recognition Workshops (CVPRW)*, pages 2923–2926, 2019. 2
- [7] E. Corona, A. Pumarola, G. Alenyà, and F. Moreno-Noguer. *Context-aware Human Motion Prediction*. 2
- [8] J. Fan, X. Shen, and Y. Wu. Scribble Tracker: A Matting-Based Approach for Robust Tracking. *IEEE Transactions on Pattern Analysis and Machine Intelligence*, 34:1633–1644, 2012. 1
- [9] K. Fragkiadaki, S. Levine, P. Felsen, and J. Malik. Recurrent Network Models for Human Dynamics. In *International Conference on Computer Vision*, 2015. 2
- [10] P. Ghosh, J. Song, E. Aksan, and O. Hilliges. Learning Human Motion Models for Long-Term Predictions. In *3DV*, 2017. 1, 2, 5
- [11] L. Gui, K. Zhang, Y. Wang, X. Liang, J. M. F. Moura, and M. Veloso. Teaching robots to predict human motion. In *2018 IEEE/RSJ International Conference on Intelligent Robots and Systems (IROS)*, 2018. 1
- [12] Golnaz Habibi, Nikita Jaipuria, and Jonathan P. How. Context-aware pedestrian motion prediction in urban intersections. *ArXiv*, 2018. 1
- [13] A. Jain, A.R. Zamir, and S. Savarese. A. adn Saxena. Structural-Rnn: Deep Learning on Spatio-Temporal Graphs. In *Conference on Computer Vision and Pattern Recognition*, 2016. 2, 5
- [14] S. Kiciroglu, H. Rhodin, S. Sinha, M. Salzmann, and P. Fua. Activemocap: Optimized Viewpoint Selection for Active Human Motion Capture. In *Conference on Computer Vision and Pattern Recognition*, 2020. 1
- [15] T. Lebailly, S. Kiciroglu, M. Salzmann, P. Fua, and W. Wang. Motion Prediction Using Temporal Inception Module. In *Asian Conference on Computer Vision*, 2020. 1, 2, 3, 5, 6
- [16] Maosen Li, Siheng Chen, Yangheng Zhao, Ya Zhang, Yanfeng Wang, and Qi Tian. Dynamic multiscale graph neural networks for 3d skeleton based human motion prediction. In *Conference on Computer Vision and Pattern Recognition*, June 2020. 2
- [17] Y. Li, L. Yuan, and N. Vasconcelos. Co-occurrence Feature Learning from Skeleton Data for Action Recognition and Detection with Hierarchical Aggregation. In *International Joint Conference on Artificial Intelligence*, 2018. 5, 10
- [18] J. Martinez, M.J. Black, and J. Romero. On Human Motion Prediction Using Recurrent Neural Networks. In *Conference on Computer Vision and Pattern Recognition*, 2017. 1, 2
- [19] J. Martinez, R. Hossain, J. Romero, and J.J. Little. A Simple Yet Effective Baseline for 3D Human Pose Estimation. In *International Conference on Computer Vision*, 2017. 5
- [20] Tomas Mikolov, Martin Karafiát, Lukas Burget, Jan Cernocký, and Sanjeev Khudanpur. Recurrent neural network based language model. volume 2, pages 1045–1048, 01 2010. 1
- [21] Romero Morais, Vuong Le, Truyen Tran, Budhaditya Saha, Moussa Mansour, and Svetha Venkatesh. Learning regularity in skeleton trajectories for anomaly detection in videos. In *CVPR*, 2019. 1
- [22] Dario Pavllo, David Grangier, and Michael Auli. Quaternet: A quaternion-based recurrent model for human motion. In *British Machine Vision Conference*, 2018. 3
- [23] Ian Simon and Sageev Oore. Performance rnn: Generating music with expressive timing and dynamics, 2017. 2
- [24] Bob Sturm, João Santos, Oded Ben-Tal, and Iryna Korshunova. Music transcription modelling and composition using deep learning. *Conference on Computer Simulation of Musical Creativity*, 04 2016. 2
- [25] Shuai Tang, Mani Golparvar-Fard, Milind Naphade, and Murari M. Gopalakrishna. Video-based motion trajectory forecasting method for proactive construction safety monitoring systems. *Journal of Computing in Civil Engineering*, 34(6), 2020. 1
- [26] Borui Wang, Ehsan Adeli, Hsu-Kuang Chiu, De-An Huang, and Juan Carlos Nieves. Imitation learning for human pose prediction. In *International Conference on Computer Vision*, pages 7123–7132, 2019. 2
- [27] Mao Wei, Liu Miaomiao, and Salzmann Mathieu. History repeats itself: Human motion prediction via motion attention. In *ECCV*, 2020. 1, 2, 3, 5, 6
- [28] Mao Wei, Liu Miaomiao, Salzmann Mathieu, and Li Hongdong. Learning trajectory dependencies for human motion prediction. In *ICCV*, 2019. 1, 2, 3, 5
- [29] J. Zhang and C. Zong. Deep neural networks in machine translation: An overview. *IEEE Intelligent Systems*, 30(5), 2015. 1, 2

6. Supplementary Material

The supplementary video which can be accessed on <https://youtu.be/GNSrwdl80GI> includes a short overview of our work. The motivation and methodology are briefly explained. We also compare videos of our qualitative results versus the results of the competing methods.

6.1. Action Recognition Model

We train two types of action recognition models: the first one being the full action classifier (FAC) and the second one the motion-only action classifier (MOAC). Their architectures are depicted in Figure 7.

Training Details The action recognition models are trained to classify sequences of 125 frames (5 seconds). Both models are trained with Adam optimizer, using a learning rate of $1e - 5$, and weight decay of $1e - 4$. In order to make the model more robust to overfitting, we have added Gaussian noise during training to the input data. With independent probabilities of 0.5, a noise of 20 mm standard deviation is added to the motion and noise of 30 mm standard deviation is added to the poses. We have found that this procedure improves the validation accuracies.

6.2. Cluster center visualization

We show a sample of 36 keypose cluster centers in Figure 8. It is necessary for them to be varied in order to be

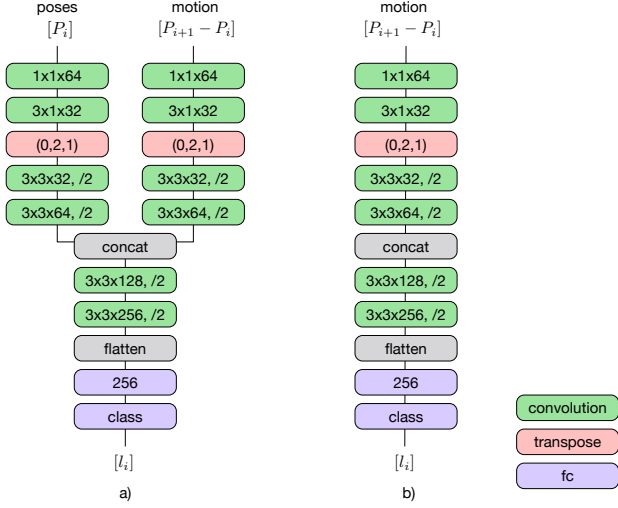


Figure 7. **Architectures used for action recognition models** Figure a) FAC architecture which takes both the poses and the motion as input in two streams and concatenates their features later on. This is identical to the model proposed in [17]. Figure b) MOAC architecture, which only takes the motion (difference between consecutive poses) as input.



Figure 8. **Visualization of keypose cluster centers.** The sampled 36 keypose cluster centers here show that the cluster centers are quite varied and are able to represent the keyposes throughout the different categories of motions.

able to express the wide range of poses seen across different action categories. We find that the keypose cluster centers include poses from many categories, such as sitting, crouching, squatting, standing, walking, and making different arm gestures.

6.3. Additional Qualitative Results

Additional qualitative results can be seen in Figures 9, 10, 11. We display the action categories which we were unable to show in our main paper due to lack of space. We again draw attention to the hand gestures our model is able to generate and the overall dynamism of the predicted motions as compared to the SOTA methods.

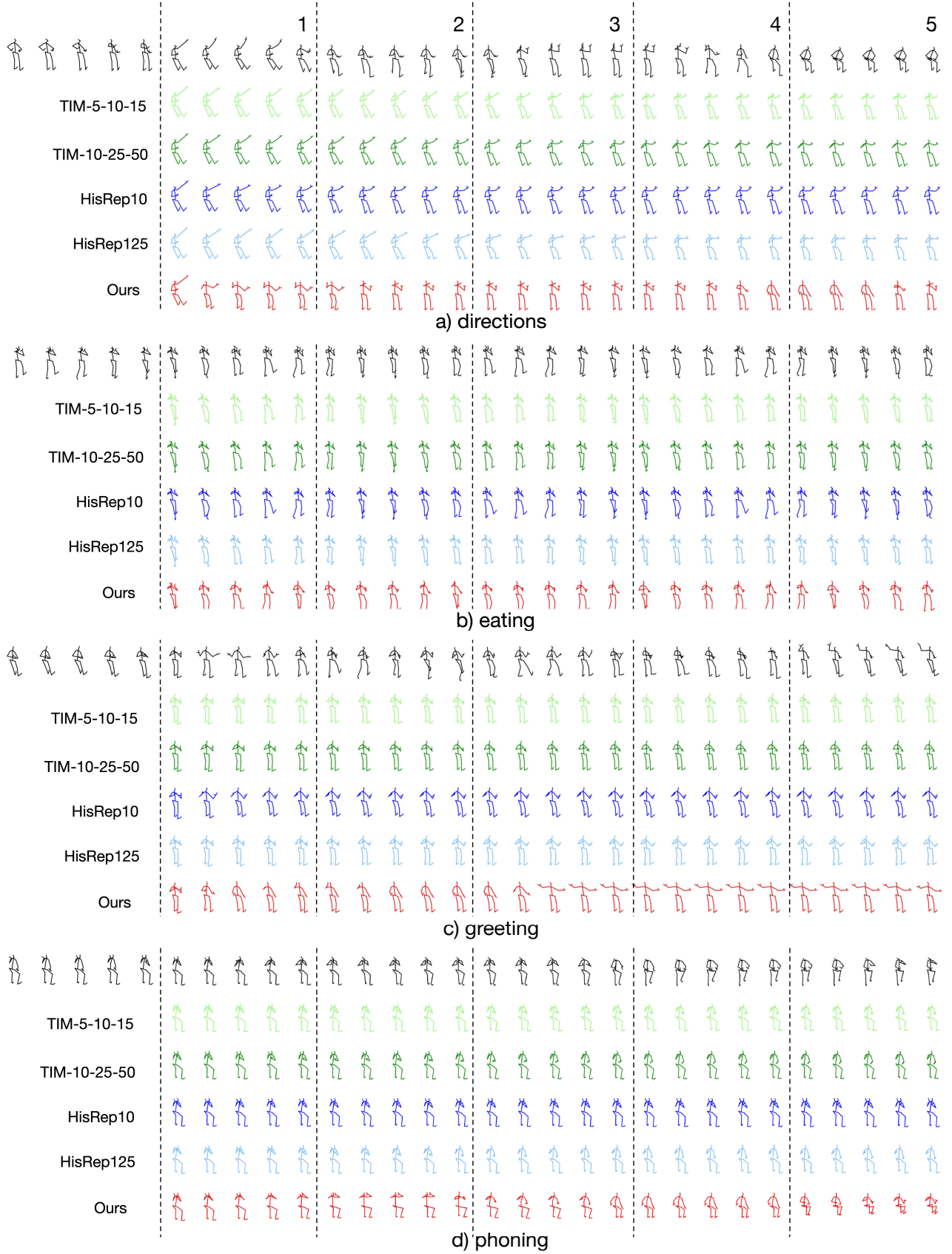


Figure 9. **Qualitative results** of actions "directions", "eating", "greeting", "phoning".

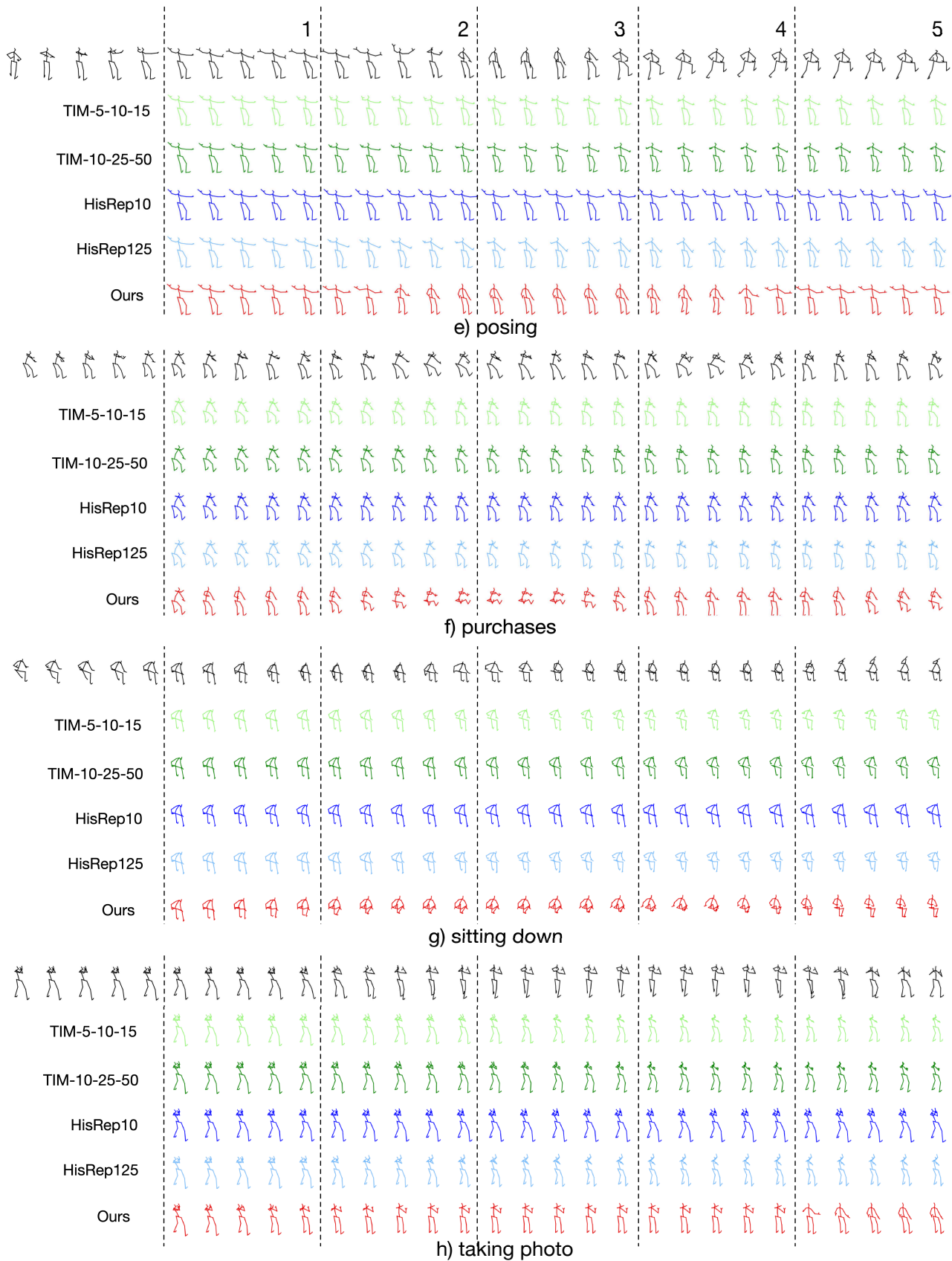


Figure 10. **Qualitative results** of actions "posing", "purchases", "sitting down", "taking photo".

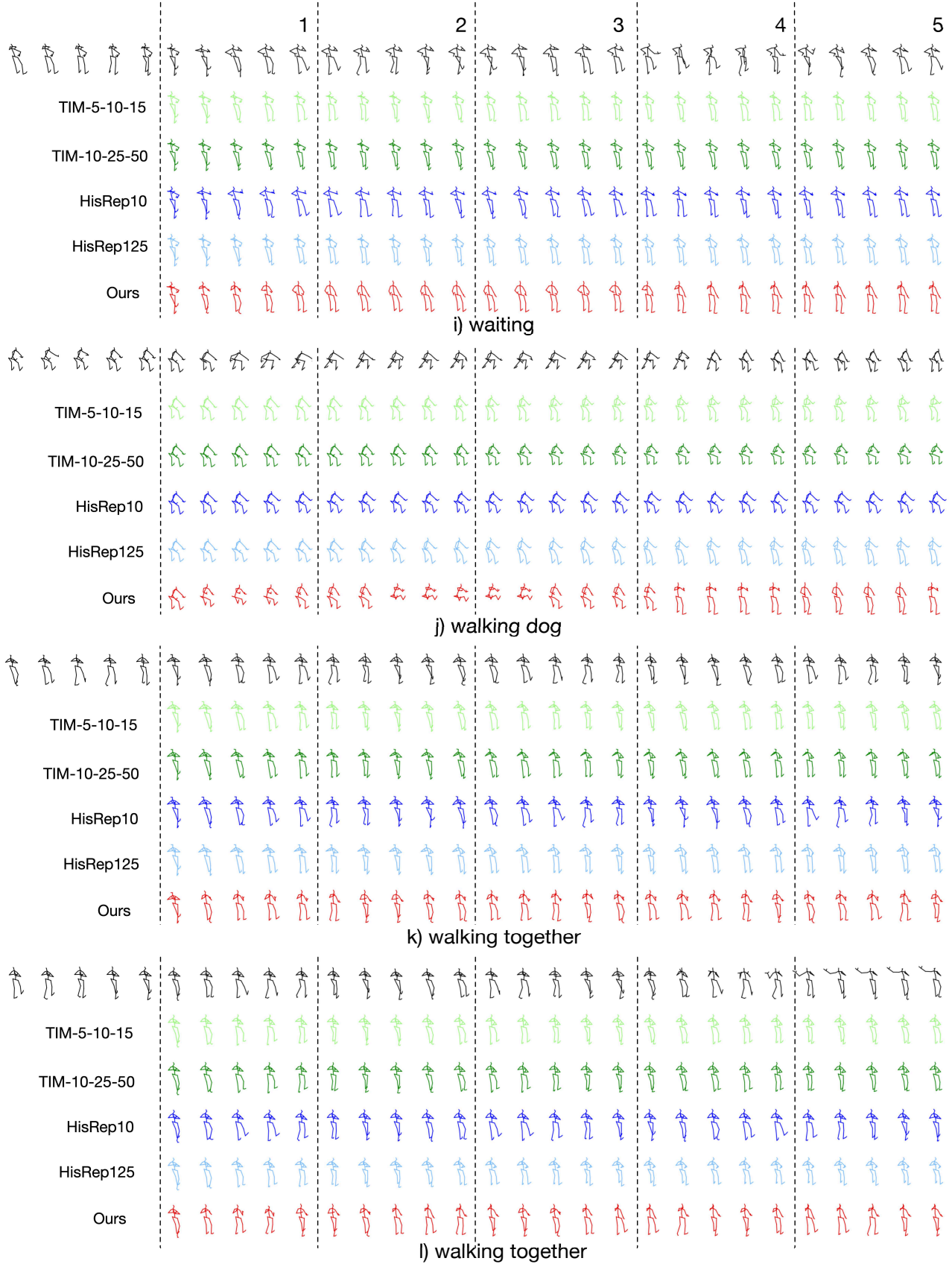


Figure 11. **Qualitative results** of actions "waiting", "walking dog", "walking together".